

Synthesis and Structural Characterization of Group 4 Metal Complexes Bearing Pentavalent Phosphorus-Bridged Ligands $[(C_{13}H_8)(^iPr_2N)P(-O)(C_2B_{10}H_{10})]^{2-}$ and $[(C_{13}H_9)(^iPr_2N)P(=O)(C_2B_9H_{10})]^{2-}$

Hong Wang,[†] Hao Shen,[†] Hoi-Shan Chan,[†] and Zuowei Xie^{*,†,‡}

Department of Chemistry, The Chinese University of Hong Kong, Shatin, New Territories, Hong Kong, People's Republic of China, and State Key Laboratory of Elemento-Organic Chemistry, Nankai University, Tianjin, People's Republic of China

Received April 8, 2008

Treatment of $(C_{13}H_9)(^iPr_2N)PCl$ with $Li_2C_2B_{10}H_{10}$ gave, after neutralization with Me_3NHCl , a trivalent phosphorus-bridged compound, $(C_{13}H_9)(^iPr_2N)P(C_2B_{10}H_{11})$. It was easily converted to a pentavalent phosphorus-bridged ligand, $(C_{13}H_9)(^iPr_2N)P(=O)(C_2B_{10}H_{11})$ (**4**), by reacting with excess hydrogen peroxide in toluene. An equimolar reaction of **4** with $Zr(NMe_2)_4$ in toluene at room temperature afforded a zirconium amide incorporating a fluorenyl unit, $[\sigma\text{-}(C_{13}H_8)(^iPr_2N)P(-O)(C_2B_{10}H_{10})]Zr(NMe_2)_2(THF)$ (**5**). Complex **5** was converted to the zirconacarborane $[\eta^1:\eta^5\text{-}(C_{13}H_9)(^iPr_2N)P(=O)(C_2B_9H_{10})]Zr(NMe_2)_2$ (**6**) in refluxing toluene in the presence of Me_2NH . Its titanium analogue, $[\eta^1:\eta^5\text{-}(C_{13}H_9)(^iPr_2N)P(=O)(C_2B_9H_{10})]Ti(NMe_2)_2$ (**7**), was directly prepared from the reaction of **4** with $Ti(NMe_2)_4$ in refluxing toluene. Complex **7** reacted with KH in C_6D_6 to generate the deprotonated product $\{[\eta^1:\eta^5\text{-}(C_{13}H_8)(^iPr_2N)P(=O)(C_2B_9H_{10})]Ti(NMe_2)_2\}(\eta^6\text{-}C_6D_6)_2K$ (**8**). These new complexes were fully characterized by various spectroscopic techniques, elemental analyses, and single-crystal X-ray diffraction studies.

Introduction

The bridging units have a large impact on the reaction chemistry of *ansa*-metallocenes.¹ Of the known bridging elements such as B, C, Si, Ge, N, and P,² the phosphorus atom is of particular interest because of its electronic and steric

properties. In principle, phosphorus-bridged ligands can exhibit a wide range of structural types, as a phosphorus atom has two common oxidation states, +3 and +5. The former is represented by the phosphine ligands $-PR-$,³ whereas the pentavalent phosphorus is found in phosphine oxides and diylides based on $-R(O=)P$ and $-R_2P<$ units, respectively.⁴ Such changes in the oxidation states would be expected to modulate the reactivity of the metal center. We recently reported phosphorus-bridged ligands $(C_9H_7)(^iPr_2N)P(C_2B_{10}H_{11})$ and $(C_9H_7)(^iPr_2N)P(=O)(C_2B_{10}H_{11})$ as well as their applications in groups 3 and 4 metal chemistry.^{5a-c} These two ligands showed very different coordination modes from group 4 metals: $[\eta^5\text{-}(C_9H_6)(^iPr_2N)P(C_2B_{10}H_{10})]M(NMe_2)_2$ ^{5b} versus $[\sigma\text{-}(C_9H_6)(^iPr_2N)P(-O)(C_2B_{10}H_{10})]Zr(NMe_2)_2$.^{5c} Stimulated by these results, we extended our research to include a fluorenyl moiety in the hope that two closely related ligands that differ in the cyclic groups will allow one to make comparisons between them. We reported here a

* Corresponding author. Fax: (852)26035057. Tel: (852)26096269. E-mail: zxie@cuhk.edu.hk.

[†] The Chinese University of Hong Kong.

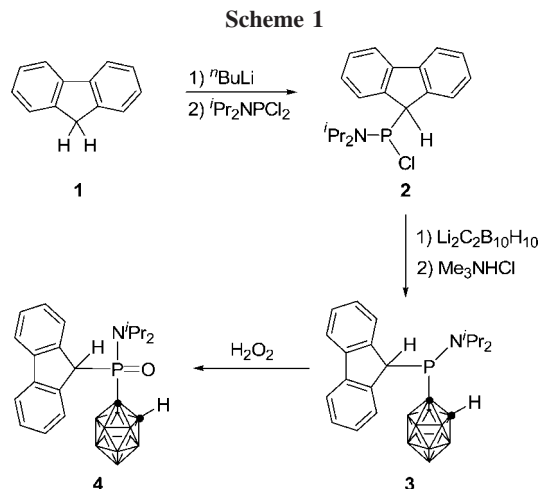
[‡] Nankai University.

(1) (a) Zachmanoglou, C. E.; Docrat, A.; Bridgewater, B. M.; Parkin, G.; Brandow, C. G.; Bercaw, J. E.; Jardine, C. N.; Lyall, M.; Green, J. C.; Keister, J. B. *J. Am. Chem. Soc.* **2002**, *124*, 9525. (b) Gladysz, J. A. (guest editor, issue 4). *Chem. Rev.* **2000**, *100*, 1167. (Special Issue on Frontiers in Metal-Catalyzed Polymerization). (c) Hosmane, N. S.; Maguire, J. A. In *Comprehensive Organometallic Chemistry III*; Crabtree, R. H., Mingos, D. M. P., Eds.; Elsevier: Oxford, 2007; Vol. 4, Chapter 3.05, p 175. (d) Chen, E. Y.-X.; Rodriguez-Delgado, A. In *Comprehensive Organometallic Chemistry III*; Crabtree, R. H., Mingos, D. M. P., Eds.; Elsevier: Oxford, 2007; Vol. 4, Chapter 4.08, p 759. (e) Kang, S. O.; Ko, J. *Adv. Organomet. Chem.* **2001**, *47*, 61. (f) Xie, Z. *Coord. Chem. Rev.* **2002**, *231*, 23. (g) Xie, Z. *Acc. Chem. Res.* **2003**, *36*, 1. (h) Xie, Z. *Coord. Chem. Rev.* **2006**, *250*, 259. (i) Deng, L.; Xie, Z. *Coord. Chem. Rev.* **2007**, *251*, 2452. (j) Teixidor, F.; Núñez, R.; Viñas, C.; Sillanpää, R.; Kivekäs, R. *Inorg. Chem.* **2001**, *40*, 2587. (k) Deng, L.; Xie, Z. *Organometallics* **2007**, *26*, 1832.

(2) (a) Durfey, D. A.; Kirss, R. U.; Frommen, C.; Feighery, W. *Inorg. Chem.* **2000**, *39*, 3506. (b) Hsu, S. C. N.; Yeh, W.-Y.; Chiang, M. Y. *J. Organomet. Chem.* **1995**, *492*, 121. (c) Sinnema, P.-J.; van der Veen, L.; Spek, A. L.; Veldman, N.; Teuben, J. H. *Organometallics* **1997**, *16*, 4245. (d) Gomes, P. T.; Green, M. L. H.; Martins, A. M. *J. Organomet. Chem.* **1998**, *551*, 133. (e) Duda, L.; Erker, G.; Fröhlich, R.; Zippel, F. *Eur. J. Inorg. Chem.* **1998**, 1153. (f) van Leusen, D.; Beetstra, D. J.; Hessen, B.; Teuben, J. H. *Organometallics* **2000**, *19*, 4084. (g) Braunschweig, H.; von Koblinski, C.; Englert, U. *Chem. Commun.* **2000**, 1049. (h) Kunz, K.; Erker, G.; Döring, S.; Fröhlich, R.; Krhr, G. *J. Am. Chem. Soc.* **2001**, *123*, 6181. (i) Kunz, K.; Erker, G.; Döring, S.; Bredeau, S.; Kehr, G.; Fröhlich, R. *Organometallics* **2002**, *21*, 1031. (j) Shapiro, P. J. *Eur. J. Inorg. Chem.* **2001**, 321. (k) Braunschweig, H.; Breitling, F. M.; Gullo, E.; Kraft, M. *J. Organomet. Chem.* **2003**, *680*, 31. (l) Aldridge, S.; Bresner, C. *Coord. Chem. Rev.* **2003**, *244*, 71. (m) Braunschweig, H.; Gross, M.; Kraft, M.; Kristen, M. O.; Leusser, D. *J. Am. Chem. Soc.* **2005**, *127*, 3282.

(3) For examples, see: (a) Barnard, T. S.; Mason, M. R. *Organometallics* **2001**, *20*, 206. (b) Malefetse, T. J.; Swiegers, G. F.; Coville, N. J.; Fernandes, M. A. *Organometallics* **2002**, *21*, 2898. (c) Kotov, V. V.; Avtomonov, E. V.; Sundermeyer, J.; Harms, K.; Lemenovskii, D. A. *Eur. J. Inorg. Chem.* **2002**, 678. (d) Ebels, J.; Pietschnig, R.; Kotila, S.; Dombrowski, A.; Niecke, E.; Nieger, M.; Schiffrer, H. M. *Eur. J. Inorg. Chem.* **1998**, 331. (e) Alt, H. G.; Jung, M. *J. Organomet. Chem.* **1998**, *568*, 127. (f) Butchard, J. R.; Curnow, O. J.; Smail, S. J. *J. Organomet. Chem.* **1997**, *541*, 407. (g) Curnow, O. J.; Huttner, G.; Smail, S. J.; Turnbull, M. M. *J. Organomet. Chem.* **1996**, *524*, 267. (h) Fallis, K. A.; Anderson, G. K.; Rath, N. P. *Organometallics* **1992**, *11*, 885. (i) Anderson, G. K.; Lin, M. *Organometallics* **1988**, *7*, 2285. (j) Anderson, G. K.; Lin, M. *Inorg. Chim. Acta* **1988**, *142*, 7.

(4) For examples, see: (a) Trinquier, G.; Ashby, M. T. *Inorg. Chem.* **1994**, *33*, 1306. (b) Schick, G.; Loew, A.; Nieger, M.; Airola, K.; Niecke, E. *Chem. Ber.* **1996**, *129*, 911. (c) Leyser, N.; Schmidt, K.; Brintzinger, H.-H. *Organometallics* **1998**, *17*, 2155. (d) Shin, J. H.; Bridgewater, B. M.; Parkin, G. *Organometallics* **2000**, *19*, 5155. (e) Brady, E. D.; Hanusa, T. P.; Pink, M.; Young, V. G., Jr. *Inorg. Chem.* **2000**, *39*, 6028. (f) Brady, E. D.; Chmely, S. C.; Jayaratne, K. C.; Hanusa, T. P.; Young, V. G., Jr. *Organometallics* **2008**, *27*, 1612.



new pentavalent phosphorus-bridged ligand $(\text{C}_{13}\text{H}_9)(^i\text{Pr}_2\text{N})\text{P}(=\text{O})(\text{C}_2\text{B}_{10}\text{H}_{11})$ (**4**) and its applications in group 4 metal chemistry. Similarities and differences in coordination chemistry between $(\text{C}_9\text{H}_7)(^i\text{Pr}_2\text{N})\text{P}(=\text{O})(\text{C}_2\text{B}_{10}\text{H}_{11})$ and $(\text{C}_{13}\text{H}_9)(^i\text{Pr}_2\text{N})\text{P}(=\text{O})(\text{C}_2\text{B}_{10}\text{H}_{11})$ are also discussed in this article.

Results and Discussion

Ligand Synthesis. The target phosphorus compound **4** contains three different substituents that have to be introduced one by one. Reaction of $^i\text{Pr}_2\text{NPCl}_2$ with 1 equiv of fluorenyl-lithium led to the isolation of $(\text{C}_{13}\text{H}_9)(^i\text{Pr}_2\text{N})\text{P}(\text{Cl})$ (**2**) in 75% yield. Compound **2** reacted subsequently with $\text{Li}_2\text{C}_2\text{B}_{10}\text{H}_{10}$ in toluene/diethyl ether (2:1) to give, after treatment with Me_3NHCl , the neutral ligand $(\text{C}_{13}\text{H}_9)(^i\text{Pr}_2\text{N})\text{P}(\text{C}_2\text{B}_{10}\text{H}_{11})$ (**3**) in 60% yield. Interaction of **3** with an excess amount of H_2O_2 in toluene at room temperature generated $(\text{C}_{13}\text{H}_9)(^i\text{Pr}_2\text{N})\text{P}(=\text{O})(\text{C}_2\text{B}_{10}\text{H}_{11})$ (**4**) in 85% yield. This oxidation reaction was clean and easily monitored by ^{31}P NMR (Scheme 1). Compounds **2–4** were fully characterized by various spectroscopic techniques and elemental analyses. The ^{31}P chemical shifts were 134.2 ppm in **2**, 85.6 ppm in **3**, and 31.8 ppm in **4**, respectively. In most cases, the ^{31}P signals of the phosphine oxides are shifted downfield from that of the corresponding phosphine.^{1j,2a,b} In contrast, the ^{31}P peak of **4** was shifted highfield, probably due to the increased $\text{N}(\text{p}_\pi) \rightarrow \text{P}(\text{d}_\pi)$ interactions. This phenomenon was also observed for the oxidation of phosphatri(3-methylindolyl)methane^{3a} and $(\text{C}_9\text{H}_7)(^i\text{Pr}_2\text{N})\text{P}(\text{C}_2\text{B}_{10}\text{H}_{11})$,^{5b,c} in which the ^{31}P resonance shifted largely highfield after being oxidized. Couplings between the phosphorus and carbon nuclei made the ^{13}C NMR spectra complicated yet interpretable. The ^{11}B NMR spectra exhibited a 3:1:2:2:2 pattern for **3** and 1:1:1:1:6 for **4**, respectively. The solid-state IR spectra showed a characteristic B–H absorption at about 2570 cm^{-1} for **3** and **4** and a unique P=O absorption at 1369 cm^{-1} for **4**.^{5c}

The molecular structure of **3** is shown in Figure 1. The geometry of the nitrogen atom is trigonal planar (sum of angles around N atom is $359.9(2)^\circ$), but the angles of $\text{C}(9)–\text{P}(1)–\text{C}(1)$, $\text{C}(1)–\text{P}(1)–\text{N}(1)$, and $\text{N}(1)–\text{P}(1)–\text{C}(9)$ ($100.8(1)^\circ$, $109.2(1)^\circ$, and $109.2(1)^\circ$) show that the coordination environment around the phosphorus atom is trigonal pyramidal. These structural data

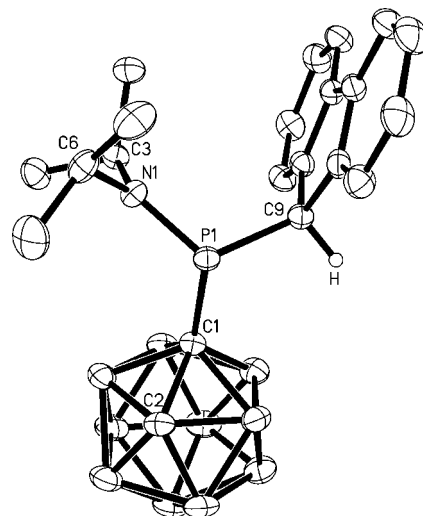


Figure 1. Molecular structure of $(\text{C}_{13}\text{H}_9)(^i\text{Pr}_2\text{N})\text{P}(\text{C}_2\text{B}_{10}\text{H}_{11})$ (**3**) (thermal ellipsoids drawn at the 30% probability level).

suggest the presence of $\text{N}(\text{p}_\pi) \rightarrow \text{P}(\text{d}_\pi)$ interactions.^{4,5} The P–C(distance) of $1.906(2) \text{ \AA}$ is very close to the corresponding value of $1.898(3) \text{ \AA}$ observed in $(\text{C}_9\text{H}_7)(^i\text{Pr}_2\text{N})\text{P}(\text{C}_2\text{B}_{10}\text{H}_{11})$,^{5a} $\sim 1.89 \text{ \AA}$ in *o*-carborane-containing *P*-chiral phosphanylferrocenes,^{5d} $1.884(6) \text{ \AA}$ in $(1\text{-Ph}_2\text{P-2-Me-1,2-C}_2\text{B}_{10}\text{H}_{10}) \cdot \text{I}_2$,^{5e} $1.892(2)/1.897(2) \text{ \AA}$ in *rac*-1,2-($^i\text{Pr}_2\text{BuCl}$)₂- $\text{C}_2\text{B}_{10}\text{H}_{10}$,^{5f} and $1.884(2)/1.893(2) \text{ \AA}$ in *meso*-1,2-($^i\text{Pr}_2\text{BuCl}$)₂- $\text{C}_2\text{B}_{10}\text{H}_{10}$,^{5f} but is longer than that of $1.811(7) \text{ \AA}$ in $[\text{NBu}_4][7\text{-P}(\text{O})\text{Ph}_2\text{-8-Ph-7,8-C}_2\text{B}_9\text{H}_{10}]$,^{1j} $1.788(2) \text{ \AA}$ in $[\text{NBu}_4][7\text{-PH}(\text{Pr})_2\text{-8-Me-7,8-C}_2\text{B}_9\text{H}_{10}]$,^{1j} and $1.804(6)/1.814(7) \text{ \AA}$ in $[\text{Cu}\{7,8\text{-}(\text{OPh})_2\text{-7,8-C}_2\text{B}_9\text{H}_{10}\}_2]$.^{5g} On the other hand, the P–C(distance) of $1.886(2) \text{ \AA}$ in **3** is close to the P–C(Bu) distance of $1.884(2)/1.877(2) \text{ \AA}$ in $1,2\text{-}(\text{P}^i\text{BuCl})_2\text{C}_2\text{B}_{10}\text{H}_{10}$,^{5f} but is longer than the P–C(distance) of $1.827(3) \text{ \AA}$ in $(\text{C}_9\text{H}_7)(^i\text{Pr}_2\text{N})\text{P}(\text{C}_2\text{B}_{10}\text{H}_{11})$ ^{5a} and the P–C(phenyl) distance of $1.824(1) \text{ \AA}$ in $1,2\text{-}(\text{PhPH})_2\text{C}_2\text{B}_{10}\text{H}_{10}$,^{5h} probably due to the different hybridization of the carbon atom bonded directly to the P atom.

The solid-state structure of **4** was further confirmed by single-crystal X-ray analyses (Figure 2). The P atom adopts a distorted tetrahedral geometry. The P=O distance of $1.466(5) \text{ \AA}$ in **4** is close to that of $1.482(2) \text{ \AA}$ in $(\text{C}_9\text{H}_7)(^i\text{Pr}_2\text{N})\text{P}(=\text{O})(\text{C}_2\text{B}_{10}\text{H}_{11})$ ^{5c} and $1.484(5) \text{ \AA}$ in the complex $[\text{NBu}_4][7\text{-P}(\text{O})\text{Ph}_2\text{-8-Ph-7,8-C}_2\text{B}_9\text{H}_{10}]$.^{1j} The geometry of the nitrogen atom in **4** is again trigonal planar (the sum of angles around the N atom is $359.9(6)^\circ$). The P–N distance of $1.630(6) \text{ \AA}$ in **4** is shorter than that of $1.661(2) \text{ \AA}$ in **3**, suggestive of a stronger $\text{N}(\text{p}_\pi) \rightarrow \text{P}(\text{d}_\pi)$ interaction in **4**, which is consistent with the ^{31}P NMR data. Table 1 compiles the key structural data for comparison.

Amide Complexes. Our previous work showed that interactions of group 4 metal dialkylamides with protioligands $\text{Me}_2\text{A}(\text{C}_5\text{H}_5)(\text{C}_2\text{B}_{10}\text{H}_{11})$,^{6a} $\text{Me}_2\text{A}(\text{C}_9\text{H}_7)(\text{C}_2\text{B}_{10}\text{H}_{11})$ ^{6a} ($\text{A} = \text{C}, \text{Si}$), and $^i\text{Pr}_2\text{NA}'(\text{C}_9\text{H}_7)(\text{C}_2\text{B}_{10}\text{H}_{11})$ ^{5b,6b} ($\text{A}' = \text{B}, \text{P}$) in toluene resulted in the clean formation of the corresponding group 4

(5) (a) Wang, H.; Wang, H.; Li, H.-W.; Xie, Z. *Organometallics* **2004**, *23*, 875. (b) Wang, H.; Chan, H.-S.; Okuda, J.; Xie, Z. *Organometallics* **2005**, *24*, 3118. (c) Wang, H.; Chan, H.-S.; Xie, Z. *Organometallics* **2006**, *25*, 2569. (d) Tschirschwitz, S.; Lönnecke, P.; Hey-Hawkins, E. *Organometallics* **2007**, *26*, 4715. (e) Núñez, R.; Farràs, P.; Teixidor, F.; Viñas, C.; Sillanpää, R.; Kivekäs, R. *Angew. Chem., Int. Ed.* **2006**, *45*, 1270. (f) Sterzik, A.; Rys, E.; Blaurock, S.; Hey-Hawkins, E. *Polyhedron* **2001**, *20*, 3007. (g) Dou, J.; Zhang, D.; Li, D.; Wang, D. *Eur. J. Inorg. Chem.* **2007**, *53*. (h) Balema, V. P.; Pink, M.; Sieler, J.; Hey-Hawkins, E.; Hennig, L. *Polyhedron* **1998**, *17*, 2087.

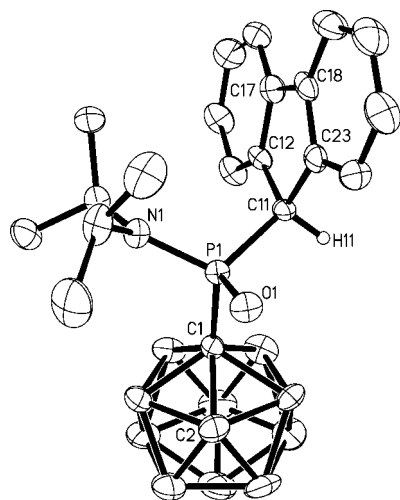


Figure 2. Molecular structure of $(C_{13}H_9)(iPr_2N)P(=O)(C_2B_{10}H_{11})$ (**4**) (thermal ellipsoids drawn at the 30% probability level).

Table 1. Selected Bond Lengths (Å) and Angles (deg) in **3–8**

(M)	3	4	5(Zr)	6(Zr)	7(Ti)	8(Ti)
P–O		1.466(5)	1.536(1)	1.534(2)	1.527(2)	1.553(2)
P–N	1.661(2)	1.630(6)	1.620(1)	1.630(3)	1.628(3)	1.650(2)
P–C(cage)	1.906(2)	1.893(8)	1.887(1)	1.807(3)	1.811(3)	1.843(3)
P–C(C ₅ ring)	1.886(2)	1.857(8)	1.713(1)	1.850(3)	1.838(3)	1.720(3)
av M–cage atom			2.343(1) ^a	2.561(4)	2.441(4)	2.447(4)
av M–N			2.001(4)	2.022(3)	1.893(3)	1.897(3)
M–O(PO)			2.089(1)	2.136(2)	2.023(2)	1.988(2)
O–P–C(cage)	104.9(3)	99.0(1)	100.1(1)	99.0(1)	96.3(1)	
O–M–C(cage)		77.4(1)				
P–O–M		137.7(1)	110.2(1)	108.6(1)	110.0(1)	

^a M–C(cage) distance.

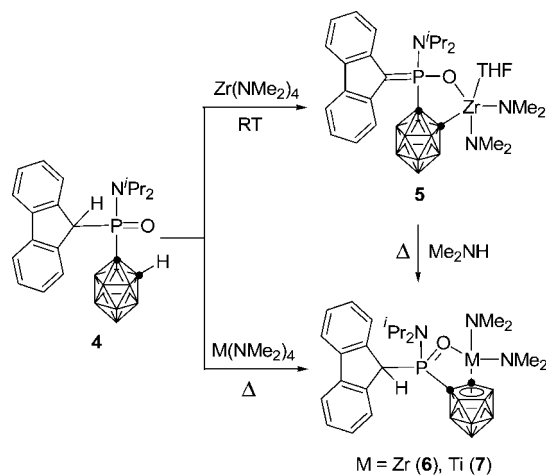
metal amide complexes.^{1h,5b,6} Group 4 metal amides $M(NR_2)_4$, however, did not react with $(C_{13}H_9)(iPr_2N)P(=O)(C_2B_{10}H_{11})$ (**3**) in toluene even at high temperatures. This result may be ascribed to the less acidic yet more sterically demanding fluorenyl functionality compared with the indenyl one.⁷ In contrast, the ¹¹B NMR experiment showed that **4** reacted readily with group 4 metal dialkylamides in C_6D_6 at room temperature to give one complex that was transformed to another one upon heating the NMR solution overnight. Accordingly, the preparative scale experiments were carried out. Treatment of **4** with 1 equiv of $Zr(NMe_2)_4$ in toluene at room temperature gave, after recrystallization from THF solution, $[\sigma\text{-}\sigma\text{-}(C_{13}H_8)(iPr_2N)P(=O)(C_2B_{10}H_{10})]Zr(NMe_2)_2(THF) \cdot THF$ (**5**·THF) in 51% yield (Scheme 2). Compound **4** showed higher reactivity over **3** owing to the high acidity of two acidic protons, sp^3 -CH of the fluorenyl and cage CH, as evidenced by their proton chemical shifts, 4.33 and 3.32 ppm in **3** vs 4.53 and 4.61 ppm in **4**. A possible reaction pathway was proposed in Scheme 3. Reaction of the two acidic protons in **4** with $Zr(NMe_2)_4$ generates the constrained-geometry complex **5'**, which isomerizes to give complex **5**. The high oxophilicity of the Zr(IV) center provides the driving force for the formation of the thermodynamically more stable product **5**. The possibility of forming the ylide intermediate **4'** cannot be ruled out at this stage.

On the other hand, the deborated product $[\eta^1\text{-}\eta^5\text{-}(C_{13}H_9)(iPr_2N)P(=O)(C_2B_9H_{10})]Zr(NMe_2)_2$ (**6**) was isolated in 55%

(6) (a) Wang, H.; Wang, Y.; Li, H.-W.; Xie, Z. *Organometallics* **2001**, *20*, 5110. (b) Zi, G.; Li, H.-W.; Xie, Z. *Organometallics* **2002**, *21*, 3850.

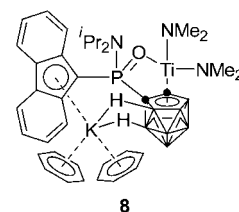
(7) (a) March, J. In *Advanced Organic Chemistry*, 4th ed.; Wiley: New York, 1992; Chapter 8, p 248. (b) Bordwell, F. G.; Bausch, M. J. *J. Am. Chem. Soc.* **1983**, *105*, 6188.

Scheme 2

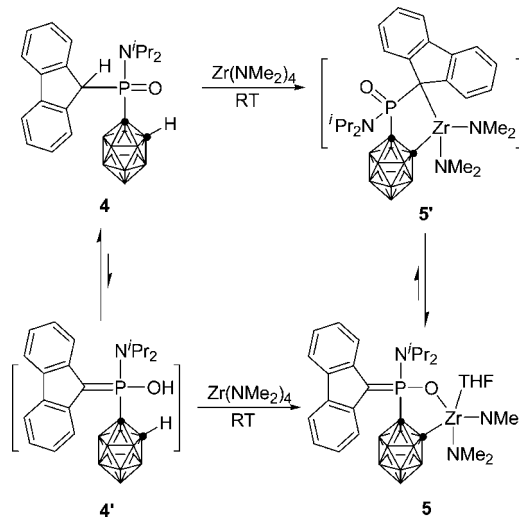


M = Zr (**6**), Ti (**7**)

KH
 C_6D_6 M = Ti



Scheme 3



yield when the above reaction was performed in toluene at 110 °C in a sealed vessel. It was noted that complex **5** was stable in refluxing toluene, but was converted to **6** in the presence of excess Me_2NH in 58% isolated yield. This result indicated that Me_2NH was essential for the transformation from **5** to **6**.^{8a} The Ti analogue, $[\eta^1\text{-}\eta^5\text{-}(C_{13}H_9)(iPr_2N)P(=O)(C_2B_9H_{10})]Ti(NMe_2)_2$ (**7**), was also prepared from **4** in 60% yield in the same manner. It was noteworthy that both **6** and **7** were stable in refluxing toluene in the absence of Me_2NH , although these molecules contain both acidic proton (from fluorenyl unit) and basic moieties (M- NMe_2 groups).

The acidic proton of the fluorenyl ring in **7** could be removed by KH. Treatment of **7** with an excess amount of KH in C_6D_6 at 80 °C for 2 days gave $\{[\eta^1\text{-}\eta^5\text{-}(C_{13}H_8)(iPr_2N)P(=O)(C_2B_9H_{10})]Ti(NMe_2)_2\} \cdot \{(\eta^5\text{-}C_6D_6)_2K\} \cdot C_6D_6$ (**8**· C_6D_6) as red crystals in 32% isolated yield. The ¹H NMR showed that the signal at 5.11

ppm corresponding to the acidic proton on the fluorenyl ring and four singlets in the range 3.22–3.64 ppm assignable to NMe₂ groups in **7** disappeared gradually, and two new singlets at 3.79 and 3.44 ppm attributable to two NMe₂ groups in **8** appeared. The ³¹P NMR resonance was shifted to highfield from 70.6 ppm in **7** to 54.8 ppm in **8**. The ¹¹B NMR spectra displayed a 1:2:2:2:1:2 pattern for **5**, 1:4:3:1 for both **6** and **7**, and 1:3:1:3:1 for **8**. The spectroscopic data of **5** were different from those of **6–8** but resembled those observed in [σ:σ-(C₉H₆)⁵(Pr₂N)-P(-O)(C₂B₁₀H₁₀)]Zr(NMe₂)₂(HNMe₂)₂.^{5c}

The P-bridged fluorenyl-dicarbollyl ligands in **6–8** are of great interest as new *ansa*-ligands in view of the unique chemical properties of (C₅Me₅)(C₂B₉H₁₁)MR and [η⁵:η⁵-Me₂C(C₅H₄)-(C₂B₉H₁₀)MCl₂]²⁻ (M = group 4 metals).⁹ We attempted to prepare this kind of hybrid ligands from **4** via selective deboration.^{9h} Many deborating reagents such as MOH/ROH (M = Na, K; R = Me, Et),¹⁰ the fluoride ion,¹¹ and various amines⁸ under different conditions were examined. All led to a mixture of products as indicated by NMR. Selective deboration of **3** and **4** was unsuccessful.

The solid-state structures of **5–8** were further confirmed by single-crystal X-ray diffraction studies and are shown in Figures 3–5, respectively. In the structure of **5**, the Zr atom is σ-bound to a bridging oxygen atom, two amido groups, and one cage carbon atom and coordinated to a THF molecule in a trigonal-bipyramidal geometry (Figure 3). All nitrogen atoms are in a trigonal-planar environment (the sum of angles around N ≈ 360°), suggesting the presence of N(p_π)→Zr(d_π) interactions. The average Zr–N distance of 2.001(4) Å is very similar to the corresponding value of 1.998(8) Å in [σ:σ-(C₉H₆)⁵(Pr₂N)-

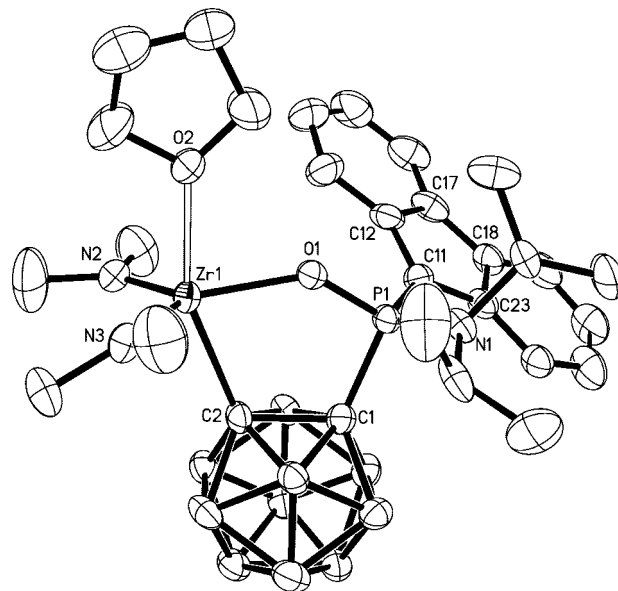


Figure 3. Molecular structure of [σ:σ-(C₁₃H₈)(Pr₂N)P(-O)-(C₂B₁₀H₁₀)]Zr(NMe₂)₂(THF) (**5**) (thermal ellipsoids drawn at the 30% probability level).

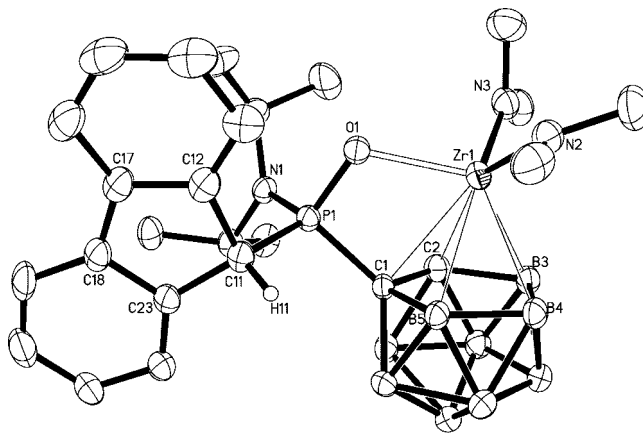


Figure 4. Molecular structure of [η¹:η⁵-(C₁₃H₉)(Pr₂N)P(=O)-(C₂B₉H₁₀)]Zr(NMe₂)₂ (**6**) (thermal ellipsoids drawn at the 30% probability level).

(8) For selective deboration by amines, see: (a) Shen, H.; Chan, H.-S.; Xie, Z. *Organometallics* **2008**, *27*, 1157. (b) Lee, Y.-J.; Lee, J.-D.; Ko, J.; Kim, S.-H.; Kang, S. O. *Chem. Commun.* **2003**, 1364. (c) Gao, M.; Tang, Y.; Xie, M.; Qian, C.; Xie, Z. *Organometallics* **2006**, *25*, 2578. (d) Wise, S. D.; Au, W.-S.; Getman, T. D. *Main Group Met. Chem.* **2002**, *25*, 411. (e) Brockman, R.; Challis, K.; Froehner, G.; Getman, T. D. *Main Group Met. Chem.* **2002**, *25*, 629. (f) Batsanov, A. S.; Goeta, A. E.; Howard, J. A. K.; Hughes, A. K.; Malget, J. M. *Dalton Trans.* **2001**, 1820. (g) Teixidor, F.; Viñas, C.; Benakki, R.; Kivekäs, R.; Sillanpää, R. *Inorg. Chem.* **1997**, *36*, 1719. (h) Laromaine, A.; Teixidor, F.; Kivekäs, R.; Sillanpää, R.; Benakki, R.; Grüner, B.; Viñas, C. *Dalton Trans.* **2005**, 1785. (i) Teixidor, F.; Gómez, S.; Lamrani, M.; Viñas, C.; Sillanpää, R.; Kivekäs, R. *Organometallics* **1997**, *16*, 1278. (j) Crespo, O.; Gimeno, M. C.; Jones, P. G.; Laguna, A. *Dalton Trans.* **1997**, 1099. (k) Viñas, C.; Butler, W. M.; Teixidor, F.; Rudolph, R. W. *Inorg. Chem.* **1986**, *25*, 4369. (l) Teixidor, F.; Viñas, C.; Abad, M. M.; Nuñez, R.; Kivekäs, R.; Sillanpää, R. *J. Organomet. Chem.* **1995**, *503*, 193. (m) Imamura, K.; Yamamoto, Y. *Bull. Chem. Soc. Jpn.* **1997**, *70*, 3103.

(9) (a) Crowther, D. J.; Baenziger, N. C.; Jordan, R. F. *J. Am. Chem. Soc.* **1991**, *113*, 1455. (b) Crowther, D. J.; Swenson, D. C.; Jordan, R. F. *J. Am. Chem. Soc.* **1995**, *117*, 10403. (c) Yoshida, M.; Crowther, D. J.; Jordan, R. F. *Organometallics* **1997**, *16*, 1349. (d) Yoshida, M.; Jordan, R. F. *Organometallics* **1997**, *16*, 4508. (e) Kreuder, C.; Jordan, R. F.; Zhang, H. *Organometallics* **1995**, *14*, 2993. (f) Bei, X.; Young, V. G., Jr.; Jordan, R. F. *Organometallics* **2001**, *20*, 355. (g) Bei, X.; Kreuder, C.; Swenson, D. C.; Jordan, R. F.; Young, V. G., Jr. *Organometallics* **1998**, *17*, 1085. (h) Wang, Y.; Liu, D.; Chan, H.-S.; Xie, Z. *Organometallics* **2008**, *27*, 2825.

(10) For examples, see: (a) Viñas, C.; Laromaine, A.; Teixidor, F.; Horáková, H.; Langauf, A.; Vespalec, R.; Mata, I.; Molins, E. *Dalton Trans.* **2007**, 3369. (b) Fox, M. A.; Goeta, A. E.; Hughes, A. K.; Johnson, A. L. *Dalton Trans.* **2002**, 2132. (c) Park, J.-S.; Kim, D.-H.; Ko, J.; Kim, S. H.; Cho, S.; Lee, C.-H.; Kang, S. O. *Organometallics* **2001**, *20*, 4632. (d) Park, J.-S.; Kim, D.-H.; Kim, S.-J.; Ko, J.; Kim, S. H.; Cho, S.; Lee, C.-H.; Kang, S. O. *Organometallics* **2001**, *20*, 4483.

(11) For examples, see: (a) Wei, X.; Carroll, P. J.; Sneddon, L. G. *Organometallics* **2006**, *25*, 609. (b) Yoo, J.; Hwang, J.-W.; Do, Y. *Inorg. Chem.* **2001**, *40*, 68. (c) Fox, M. A.; Gill, W. R.; Herbertson, P. L.; MacBride, J. A. H.; Wade, K.; Colquhoun, H. M. *Polyhedron* **1996**, *15*, 565. (d) Tomita, H.; Luu, H.; Onak, T. *Inorg. Chem.* **1991**, *30*, 812. (e) Fox, M. A.; MacBride, J. A. H.; Wade, K. *Polyhedron* **1997**, *16*, 2499. (f) Fox, M. A.; Wade, K. *Polyhedron* **1997**, *16*, 2517. (g) Fox, M. A.; Wade, K. *J. Organomet. Chem.* **1999**, *573*, 279.

P(-O)(C₂B₁₀H₁₀)]Zr(NMe₂)₂(HNMe₂)₂,^{5c} 2.010(6) Å in [σ:η⁵-(C₉H₆)-(C₂B₉H₁₀)]Zr(NMe₂)(DME),^{8a,12} 2.006(4) Å in [σ:η⁵-{[3-C(=CPh₂)-O]C₉H₆}(C₂B₉H₁₀)]Zr(NMe₂)(THF)₂,^{8a} 2.005(7) Å in (μ-O)[Zr(NMe₂)(O-Ar)₂]₂ (Ar = 2,6-Bu₂-4-Me-3,5-N₂C₄),¹³ and 2.025(4) Å in [η⁵-(Bn₂NCH₂CH₂)(C₂B₉H₁₀)]Zr(NMe₂)₂-(HNMe₂) (Bn = C₆H₅CH₂).¹⁴ The bond distances of Zr–O, Zr–C(cage), P–O, P=C, and P–N in **5** (Table 1) are almost identical with those values observed in its indenyl derivative.^{5c}

Complexes **6** and **7** are isostructural and isomorphous. The representative structure of **6** is shown in Figure 4. The metal atom is η⁵-bound to the dicarbollyl and σ-bound to two amido groups and one bridging oxygen atom in a three-legged piano-stool geometry. The short M–N(2) and M–N(3) distances (2.030(3) and 2.014(3) Å in **6**, 1.901(3) and 1.885(3) Å in **7**) and the planar geometry around N(2) and N(3) indicate that both nitrogen atoms with sp² hybridization are engaged in

(12) Shen, H.; Chan, H.-S.; Xie, Z. *J. Am. Chem. Soc.* **2007**, *129*, 12934.

(13) Lee, A. V.; Schafer, L. L. *Organometallics* **2006**, *25*, 5249.

(14) Lee, Y.-J.; Lee, J.-D.; Jeong, H.-J.; Son, K.-C.; Ko, J.; Cheong, M.; Kang, S. O. *Organometallics* **2005**, *24*, 3008.

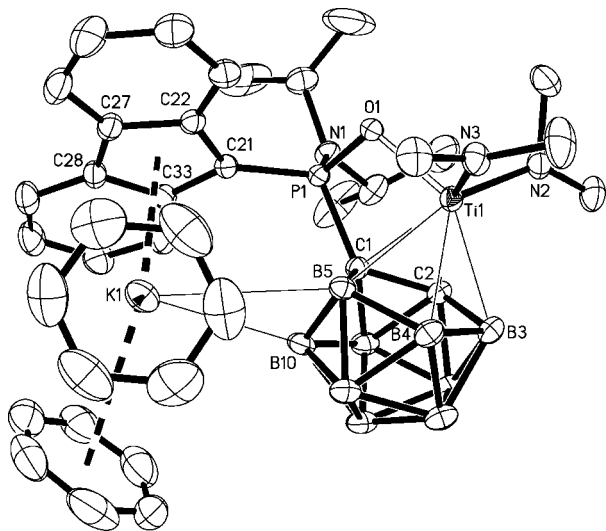


Figure 5. Molecular structure of $\{[\eta^1:\eta^5-(C_{13}H_8)(^iPr_2N)P(=O)-(C_2B_9H_{10})]Ti[(NMe_2)_2]\}\{\eta^6-C_6D_6\}_2K$ (**8**) (thermal ellipsoids drawn at the 30% probability level).

$N(p_\pi) \rightarrow M(d_\pi)$ interactions. The P–C(cage) distances of 1.807(3) Å in **6** and 1.811(3) Å in **7** are close to that of 1.811(7) Å in $[7-P(O)Ph_2-8-Ph-7,8-C_2B_{10}H_{10}]^-$,^{1j} but are shorter than that of 1.887(6) Å in $[\eta^5:\sigma-(C_9H_6)(^iPr_2N)P(C_2B_{10}H_{10})]Zr(NMe_2)_2$,^{5b} 1.867(8) Å in $[\sigma:\sigma-(C_9H_6)(^iPr_2N)P(O)(C_2B_{10}H_{10})]Zr(NMe_2)_2$,^{5c} and ~1.89 Å in *o*-carborane-containing *P*-chiral phosphanylferrocenes.^{5d} The P–O distances of 1.534(2) Å in **6** and 1.527(2) Å in **7** are comparable to that of 1.518(3) Å observed in $TiCl_4[OP(C_5H_{10}N)_3]_2$,¹⁵ but are significantly longer than the 1.466(5) Å in **4** and 1.484(5) Å in $[7-P(O)Ph_2-8-Ph-7,8-C_2B_{10}H_{10}]^-$,^{1j} suggestive of a strong interaction between P=O and M. The Zr–N distance of 2.022(3) Å, Zr–O distance of 2.136(2) Å, and P–C(ring) distance of 1.850(3) Å in **6** are longer than those in **5**. The average Zr–cage atom distance of 2.561(4) Å in **6** can be compared to that of 2.530(4) Å in $[\eta^5-(C_9H_7)(C_2B_9H_{10})]Zr(NMe_2)_2(HNMe_2)$,^{8a} 2.605(3) Å in $[\eta^5-(Me_2NCH_2)(C_2B_9H_{10})]Zr(NMe_2)_2(HNMe_2)$,¹⁶ and 2.546(5) Å in $[\eta^5-(Bn_2NCH_2CH_2)(C_2B_9H_{10})]Zr(NMe_2)_2(HNMe_2)$ (Bn = $C_6H_5CH_2$).¹⁴ The average Ti–cage atom distance of 2.441(4) Å in **7** is longer than that of 2.365(4) Å in $[\sigma:\eta^1:\eta^5-(OCH_2)-(Me_2NCH_2)(C_2B_9H_9)]Ti(NMe_2)$,¹⁷ 2.350(4) Å in $[\sigma:\eta^5-(C_9H_6)-(C_2B_9H_{10})]Ti(NMe_2)(DME)$,^{8a} 2.398(8) Å in $[\eta^1:\eta^5-(Me_2NCH_2)-(C_2B_9H_{10})]Ti(NMe_2)$,¹⁶ and 2.413(5) Å in $[\eta^5-(Bn_2NCH_2CH_2)(C_2B_9H_{10})]Ti(NMe_2)_2(HNMe_2)$ (Bn = $C_6H_5CH_2$).¹⁴

The molecular structure of **8** is composed of the cation $[K(C_6D_6)_2]^+$ and the anion $\{[\eta^1:\eta^5-(C_{13}H_8)(^iPr_2N)P(=O)-(C_2B_9H_{10})]Ti[(NMe_2)_2]\}^-$, which are associated with each other through two B–H···K interactions (Figure 5). The K atom is also bound to the five-membered ring of the fluorenyl ligand in an η^5 -fashion. In addition, the K atom is asymmetrically bound to the two C_6D_6 molecules in an η^6 -fashion. The average $K \cdots BH$ (3.357(4) Å) and $K \cdots C$ (3.317(5) Å) distances are comparable to the literature data.¹⁸ As shown in Table 1, the coordination geometry and the distances around the Ti atom in **8** are very close to those in **7**. However, the coordination

environment around P is dramatically changed. The P–C(ring) distance of 1.720(3) Å in **8** is significantly shorter than that of 1.838(3) Å in **7** and is very close to the P=C double-bond distance of 1.713(1) Å observed in **5**. The geometry of the ring carbon that is directly bonded to the P atom is also changed from a distorted tetrahedron to a trigonal plane.

Conclusion

Two new trivalent and pentavalent phosphorus-bridged fluorenyl-carboranyl ligands, $(C_{13}H_9)(^iPr_2N)P(C_2B_{10}H_{11})$ and $(C_{13}H_9)(^iPr_2N)P(=O)(C_2B_{10}H_{11})$, were synthesized and fully characterized. They showed a significantly different reactivity pattern. The former did not react with $M(NMe_2)_4$, whereas the latter reacted readily with $M(NMe_2)_4$ to give the amine elimination product $[\sigma:\sigma-(C_{13}H_8)(^iPr_2N)P(O)(C_2B_{10}H_{10})]Zr(NMe_2)_2(THF)$ (**5**) at room temperature or the amine elimination/deboration complexes $[\eta^1:\eta^5-(C_{13}H_9)(^iPr_2N)P(=O)-(C_2B_9H_{10})]M(NMe_2)_2$ (M = Zr (**6**), Ti (**7**)) at higher temperature. The stronger acidity of two acidic protons in **4** over **3** or the formation of ylide **4'** was suggested to provide the driving force for amine elimination reaction. The presence of Me_2NH proved to be essential for the deboration reaction to proceed. The acidic proton on the fluorenyl ring in **7** could be removed by excess KH, resulting in the isolation of the corresponding deprotonated product $\{[\eta^1:\eta^5-(C_{13}H_8)(^iPr_2N)P(=O)(C_2B_9H_{10})]Ti[(NMe_2)_2]\}(\eta^6-C_6D_6)_2K$ (**8**).

Experimental Section

General Procedures. All experiments were performed under an atmosphere of dry nitrogen with the rigid exclusion of air and moisture using standard Schlenk or cannula techniques, or in a glovebox. All organic solvents were freshly distilled from sodium benzophenone ketyl immediately prior to use. $Li_2C_2B_{10}H_{10}$ was prepared according to literature methods.¹⁹ $M(NMe_2)_4$ (M = Ti, Zr) and other chemicals were purchased from Aldrich Chemical Co. and used as received unless otherwise noted. Infrared spectra were obtained from KBr pellets prepared in the glovebox on a Perkin-Elmer 1600 Fourier transform spectrometer. ¹H NMR spectra were recorded on a Bruker DPX 300 spectrometer at 300.0 MHz. ¹³C NMR spectra were recorded on a Bruker DPX 300 spectrometer at 75.5 MHz or a Varian Inova 400 spectrometer at 100.7 MHz. ¹¹B and ³¹P NMR spectra were recorded on a Varian Inova 400 spectrometer at 128.3 and 161.9 MHz, respectively. All chemical shifts are reported in δ units with reference to the residual protons and carbons of the deuterated solvents for proton and carbon chemical shifts, to external $BF_3 \cdot OEt_2$ (0.00 ppm) for boron chemical shifts, and to external 85% H_3PO_4 (0.00 ppm) for phosphorus chemical shifts. Elemental analyses were performed by MEDAC Ltd., U.K., or Shanghai Institute of Organic Chemistry, CAS, China.

Preparation of $(C_{13}H_9)(^iPr_2N)PCL$ (2**).** A 1.6 M solution of $nBuLi$ in *n*-hexane (31.5 mL, 50.4 mmol) was added dropwise to a diethyl ether solution (250 mL) of fluorene (5.76 g, 50.0 mmol) at $-78^\circ C$, and the mixture was stirred at room temperature for 6 h. The precipitate ($C_{13}H_9Li$) was collected by filtration, washed with *n*-hexane (50 mL \times 2), and dried under vacuum. This white solid was dissolved in diethyl ether (100 mL) and added dropwise to a hexane solution (300 mL) of $(^iPr_2N)PCL_2$ (15.15 g, 75.0 mmol) at $-78^\circ C$ with stirring. The reaction mixture was then stirred overnight at room temperature. After filtration, the solvent and excess $(^iPr_2N)PCL_2$ were removed under vacuum, giving a brown, oily residue. Recrystallization from *n*-hexane afforded **2** as a yellow, crystalline solid (12.59 g, 75%). ¹H NMR (C_6D_6): δ 8.04 (d, *J* =

(15) Winter, C. H.; Lewkebandara, T. S.; Proscia, J. W.; Rheingold, A. L. *Inorg. Chem.* **1994**, *33*, 1227.

(16) Lee, J.-D.; Lee, Y.-J.; Son, K.-C.; Cheong, M.; Ko, J.; Kang, S. O. *Organometallics* **2007**, *26*, 3374.

(17) Shen, H.; Chan, H.-S.; Xie, Z. *Organometallics* **2007**, *26*, 2694.

(18) (a) Chui, K.; Li, H.-W.; Xie, Z. *Organometallics* **2000**, *19*, 5447.

(b) Deng, L.; Xie, Z. *Organometallics* **2007**, *26*, 1832.

(19) Gomez, F. A.; Hawthorne, M. F. *J. Org. Chem.* **1992**, *57*, 1384.

Table 2. Crystal Data and Summary of Data Collection and Refinement for **3**, **4**, and **5**·THF

	3	4	5 ·THF
formula	C ₂₁ H ₃₄ B ₁₀ NP	C ₂₁ H ₃₄ B ₁₀ NOP	C ₃₃ H ₆₀ B ₁₀ N ₃ O ₃ PZr
cryst size (mm)	0.60 × 0.20 × 0.10	0.40 × 0.30 × 0.20	0.30 × 0.20 × 0.10
fw	439.6	455.6	777.1
cryst syst	monoclinic	monoclinic	monoclinic
space group	<i>P</i> 2 ₁ / <i>n</i>	<i>P</i> 2 ₁ / <i>n</i>	<i>P</i> 2 ₁ / <i>n</i>
<i>a</i> , Å	11.294(1)	11.290(1)	9.036(1)
<i>b</i> , Å	11.059(1)	10.956(1)	26.326(2)
<i>c</i> , Å	20.992(1)	21.116(2)	17.607(1)
β, deg	105.00(1)	105.09(1)	95.73(1)
<i>V</i> , Å ³	2532.6(2)	2522.0(4)	4167.2(5)
<i>Z</i>	4	4	4
<i>D</i> _{calcd} , Mg/m ³	1.153	1.200	1.239
radiation (λ), Å	Mo Kα (0.71073)	Mo Kα (0.71073)	Mo Kα (0.71073)
2θ range, deg	3.8 to 56.1	3.8 to 50.0	2.8 to 50.0
μ, mm ⁻¹	0.120	0.125	0.338
<i>F</i> (000)	928	960	1632
no. of obsd reflns	6083	3946	6539
no. of params refnd	298	307	460
goodness of fit	1.010	1.136	1.017
R1	0.049	0.109	0.093
wR2	0.118	0.244	0.231

Table 3. Crystal Data and Summary of Data Collection and Refinement for **6**, **7**·CH₃CN, and **8**·C₆D₆

	6	7 ·CH ₃ CN	8 ·C ₆ D ₆
formula	C ₂₅ H ₄₅ B ₉ N ₃ OPZr	C ₂₇ H ₄₈ B ₉ N ₄ OPTi	C ₄₃ H ₄₄ B ₉ D ₁₈ KN ₃ OPTi
cryst size (mm)	0.20 × 0.20 × 0.15	0.20 × 0.10 × 0.05	0.50 × 0.40 × 0.20
fw	623.1	620.9	870.3
cryst syst	triclinic	triclinic	monoclinic
space group	<i>P</i> $\bar{1}$	<i>P</i> $\bar{1}$	<i>P</i> 2 ₁ / <i>n</i>
<i>a</i> , Å	10.590(3)	10.172(2)	10.509(1)
<i>b</i> , Å	11.642(3)	10.490(1)	26.748(1)
<i>c</i> , Å	13.723(4)	18.189(2)	17.105(1)
α, deg	87.65(1)	104.14(1)	90
β, deg	70.19(1)	91.39(1)	100.61(1)
γ, deg	83.51(1)	111.63(1)	90
<i>V</i> , Å ³	1581.6(8)	1735.5(2)	4726.0(3)
<i>Z</i>	2	2	4
<i>D</i> _{calcd} , Mg/m ³	1.308	1.188	1.198
radiation (λ), Å	Mo Kα (0.71073)	Mo Kα (0.71073)	Mo Kα (0.71073)
2θ range, deg	3.5 to 50.0	2.3 to 50.0	2.9 to 52.0
μ, mm ⁻¹	0.423	0.320	0.339
<i>F</i> (000)	648	656	1800
no. of obsd reflns	5483	6072	9263
no. of params refnd	369	388	532
goodness of fit	0.991	1.002	1.029
R1	0.049	0.062	0.062
wR2	0.124	0.159	0.171

6.9 Hz, 1H, fluorenyl), 7.84 (d, *J* = 6.9 Hz, 1H, fluorenyl), 7.60 (t, *J* = 6.9 Hz, 2H, fluorenyl), 7.20 (m, 4H, fluorenyl), 4.54 (d, ²*J*_{H-P} = 9.3 Hz, 1H, fluorenyl), 3.14 (m, 2H, NCH(CH₃)₂), 1.08 (brs, 6H, NCH(CH₃)₂), 0.61 (brs, 6H, NCH(CH₃)₂). ¹³C NMR (C₆D₆): δ 143.1, 142.1, 127.1, 127.0, 126.7, 120.2, 54.6 (d, ¹*J*_{-P} = 44.0 Hz) (C₁₃H₉), 50.1 (br), 46.9 (br) (N(CH(CH₃)₂)), 31.9, 23.0, 14.5, 1.61 (NCH(CH₃)₂). ³¹P{¹H} NMR (C₆D₆): δ 134.2. IR (KBr, cm⁻¹): ν 3058 (br), 2966 (vs), 2928 (vs), 1443 (vs), 1364 (s), 1148 (vs), 1117 (vs), 1009 (s), 960 (vs), 867 (m), 793 (s), 743 (vs). Anal. Calcd for C₁₉H₂₃ClNP (**2**): C, 68.77; H, 6.99; N, 4.22. Found: C, 68.56; H, 6.63; N, 4.40.

Preparation of (C₁₃H₉)(^tPr₂N)P(C₂B₁₀H₁₁) (3**).** A Et₂O solution (30 mL) of **2** (3.32 g, 10.0 mmol) was added dropwise to a suspension of Li₂C₂B₁₀H₁₀ (10.0 mmol) in toluene/Et₂O (2:1, v/v, 30 mL) at -78 °C. The reaction mixture was then stirred at room temperature overnight. After addition of an aqueous solution (30 mL) of Me₃NHCl (1.91 g, 20.0 mmol), the organic layer was separated, washed with water (10 mL × 1) and subsequently a saturated solution of NaCl (10 mL × 1), and dried with anhydrous Na₂SO₄. Removal of the solvents afforded a pale yellow solid. Recrystallization from *n*-hexane gave **3** as colorless crystals (2.64 g, 60%). ¹H NMR (C₆D₆): δ 8.11 (d, *J* = 9.0 Hz, 1H, fluorenyl),

7.56 (d, *J* = 6.9 Hz, 2H, fluorenyl), 7.21 (m, 3H, fluorenyl), 7.05 (m, 2H, fluorenyl), 4.33 (s, 1H, fluorenyl), 3.32 (br, 1H, cage CH), 2.37 (m, 2H, NCH(CH₃)₂), 0.13 (d, *J* = 6.0 Hz, 6H, NCH(CH₃)₂), -0.20 (d, *J* = 6.0 Hz, 6H, NCH(CH₃)₂). ¹³C NMR (C₆D₆): δ 142.6, 142.0, 140.3, 128.7, 127.9, 127.2, 127.1, 126.5, 126.3, 126.2, 120.1, 119.4, 44.4 (d, ¹*J*_{-P} = 55.6 Hz) (C₁₃H₉), 79.2 (d, ¹*J*_{-P} = 56.9 Hz), 67.9 (cage C), 52.7 (br), 50.7 (br) (NCH(CH₃)₂), 25.0, 24.1, 21.1, 20.8 (NCH(CH₃)₂). ¹¹B{¹H} NMR (C₆D₆): δ -0.7 (3B), -6.4 (1B), -7.9 (2B), -10.8 (2B), -12.7 (2B). ³¹P{¹H} NMR (C₆D₆): δ 85.6. IR (KBr, cm⁻¹): ν 2594 (vs) (B-H). Anal. Calcd for C₂₁H₃₄B₁₀NP (**3**): C, 57.38; H, 7.80; N, 3.19. Found: C, 57.12; H, 7.61; N, 2.96.

Preparation of (C₁₃H₉)(^tPr₂N)P(=O)(C₂B₁₀H₁₁) (4**).** An excess amount of hydrogen peroxide (30% aqueous solution, 2.0 mL, 17.0 mmol) was added to a toluene solution (10 mL) of **3** (439 mg, 1.0 mmol) at room temperature, and the mixture was stirred for two days. The organic layer was collected and washed with a saturated solution of Na₂S₂O₃ (15 mL × 2), NaHCO₃ (15 mL × 2), and NaCl (20 mL × 2), respectively. Removal of the solvent afforded a white solid. Recrystallization from toluene gave **4** as colorless crystals (344 mg, 85%). ¹H NMR (C₆D₆): δ 8.35 (d, *J* = 6.0 Hz, 1H, fluorenyl), 7.96 (d, *J* = 7.8 Hz, 1H, fluorenyl), 7.49 (m, 2H, fluorenyl), 7.20 (m, 2H, fluorenyl), 6.99 (m, 2H, fluorenyl), 4.61

(br, 1H, cage CH), 4.53 (d, $^2J_{H-P} = 23.4$ Hz, 1H, fluorenyl), 2.81 (m, 2H, NCH(CH₃)₂), 0.90 (d, $J = 6.0$ Hz, 6H, NCH(CH₃)₂), 0.10 (d, $J = 6.0$ Hz, 6H, NCH(CH₃)₂). ¹³C NMR (C₆D₆): δ 143.8, 141.5, 138.5, 130.5, 127.8, 127.1, 125.7, 120.3, 119.4, 52.2 (d, $^1J_{-P} = 47.4$ Hz) (C₁₃H₉), 76.4 (d, $^1J_{-P} = 54.6$ Hz), 65.8 (cage C), 47.8 (br) (NCH(CH₃)₂), 30.1, 22.5 (NCH(CH₃)₂). ¹¹B{¹H} NMR (C₆D₆): δ -0.8 (1B), -3.0 (1B), -7.6 (1B), -8.6 (1B), -13.4 (6B). ³¹P{¹H} NMR (C₆D₆): δ 31.8. IR (KBr, cm⁻¹): ν 2596 (vs) (B-H), 1369 (s) (P=O). Anal. Calcd for C₂₁H₃₄B₁₀NOP (4): C, 55.36; H, 7.52; N, 3.07. Found: C, 55.15; H, 7.60; N, 2.98.

Preparation of $[\sigma\text{-}(\text{C}_{13}\text{H}_9)(\text{Pr}_2\text{N})\text{P}(\text{O})(\text{C}_2\text{B}_9\text{H}_{10})]\text{Zr}(\text{NMe}_2)_2 \cdot (\text{THF}) \cdot \text{THF}$ (5 · THF). A toluene solution (10 mL) of **4** (455 mg, 1.0 mmol) was slowly added to a toluene solution (10 mL) of Zr(NMe₂)₄ (267 mg, 1.0 mmol) at -78 °C, and the reaction mixture was slowly warmed to room temperature and stirred for 3 h. After removal of the solvent, the residue was extracted with a mixed solvent of THF/*n*-hexane (2:1, v/v, 10 mL × 2). The organic solutions were combined and concentrated to dryness, affording a pale yellow solid. Recrystallization from THF/*n*-hexane at -30 °C gave **5 · THF** as pale yellow crystals (396 mg, 51%). ¹H NMR (C₆D₆): δ 8.77 (d, $J = 7.8$ Hz, 1H, fluorenyl), 8.32 (m, 2H, fluorenyl), 7.75 (m, 1H, fluorenyl), 7.66 (t, $J = 7.8$ Hz, 1H, fluorenyl), 7.33 (t, $J = 7.8$ Hz, 1H, fluorenyl), 7.18 (m, 2H, fluorenyl), 3.72 (m, 2H, NCH(CH₃)₂), 3.66 (m, 8H, THF), 2.53 (s, 6H, N(CH₃)₂), 1.75 (s, 6H, N(CH₃)₂), 1.66 (m, 8H, THF), 1.25 (d, $J = 6.6$ Hz, 6H, NCH(CH₃)₂), 0.83 (d, $J = 6.6$ Hz, 6H, NCH(CH₃)₂). ¹³C NMR (C₆D₆): δ 144.2, 138.9, 132.2, 130.4, 124.9, 121.2, 120.8, 119.6, 117.9, 116.9, 116.7, 72.8 (d, $^1J_{-P} = 159.0$ Hz) (C₁₃H₉), 95.0 (cage C), 67.9, 22.9 (THF), 48.6 (br), 37.9 (br) (NCH(CH₃)₂), 41.4, 40.5 (N(CH₃)₂), 31.8, 25.7, 23.7, 22.7 (NCH(CH₃)₂). ¹¹B{¹H} NMR (C₆D₆): δ -2.0 (1B), -0.1 (2B), -2.8 (2B), -6.1 (2B), -7.3 (1B), -10.6 (2B). ³¹P{¹H} NMR (C₆D₆): δ 48.1. IR (KBr, cm⁻¹): ν 2568 (vs) (B-H). Anal. Calcd for C₃₁H₅₆B₁₀N₃O_{2.5}PZr (5 + 0.5THF): C, 50.24; H, 7.62; N, 5.67. Found: C, 50.19; H, 7.50; N, 5.52.

Preparation of $[\eta^1\text{-}\eta^5\text{-}(\text{C}_{13}\text{H}_9)(\text{Pr}_2\text{N})\text{P}(\text{O})(\text{C}_2\text{B}_9\text{H}_{10})]\text{Zr}(\text{NMe}_2)_2$ (6). A toluene solution (20 mL) of **5** (398 mg, 0.5 mmol) and Me₂NH (0.15 mL, 2.3 mmol) in a sealed Schlenk flask was heated to 80 °C for 10 h to give a clear orange solution, which was concentrated to about 8 mL. *n*-Hexane diffusion into the resulting solution over a week gave **6** as yellow crystals (181 mg, 58%). ¹H NMR (C₆D₆): δ 8.09 (d, $J = 7.8$ Hz, 1H, fluorenyl), 7.93 (d, $J = 6.0$ Hz, 1H, fluorenyl), 7.42 (m, 2H, fluorenyl), 7.12 (m, 3H, fluorenyl), 6.92 (t, $J = 6.0$ Hz, 1H, fluorenyl), 5.10 (d, $^1J_{H-P} = 15.9$ Hz, 1H, fluorenyl), 3.36 (s, 6H, N(CH₃)₂), 3.10 (s, 6H, N(CH₃)₂), 2.65 (m, 2H, NCH(CH₃)₂), 0.52 (d, $J = 6.0$ Hz, 6H, NCH(CH₃)₂), -0.15 (d, $J = 6.0$ Hz, 6H, NCH(CH₃)₂). ¹³C NMR (C₆D₆): δ 143.2, 142.4, 137.3, 136.7, 127.1, 120.1, 48.9 (d, $^1J_{-P} = 74.0$ Hz) (C₁₃H₉), 89.0 (cage C), 48.0 (br) (NCH(CH₃)₂), 50.6, 47.0 (N(CH₃)₂), 31.7, 23.0, 22.2, 21.3 (NCH(CH₃)₂). ¹¹B{¹H} NMR (C₆D₆): δ 7.4 (1B), -1.3 (4B), -12.5 (3B), -17.7 (1B). ³¹P{¹H} NMR (C₆D₆): δ 70.0. IR (KBr, cm⁻¹): ν 2531 (vs) (B-H), 1435 (s) (P=O). Anal. Calcd for C₂₅H₄₅B₉N₃OPZr (6): C, 48.19; H, 7.28; N, 6.74. Found: C, 48.21; H, 7.33; N, 6.81.

Alternate Method. Complex **6** was also prepared in 55% isolated yield from **4** (455 mg, 1.0 mmol) and Zr(NMe₂)₄ (267 mg, 1.0 mmol) in a sealed Schlenk flask in refluxing toluene (20 mL) using the same procedures mentioned above.

Preparation of $[\eta^1\text{-}\eta^5\text{-}(\text{C}_{13}\text{H}_9)(\text{Pr}_2\text{N})\text{P}(\text{O})(\text{C}_2\text{B}_9\text{H}_{10})]\text{Ti}(\text{NMe}_2)_2 \cdot \text{CH}_3\text{CN}$ (7 · CH₃CN). A toluene solution (10 mL) of **4** (455 mg, 1.0 mmol) was slowly added to a toluene solution (10 mL) of Ti(NMe₂)₄ (225 mg, 1.0 mmol) at room temperature with stirring. The reaction mixture was then heated to reflux overnight to give a dark red solution. Removal of the solvent yielded a dark

red solid. Recrystallization from toluene/CH₃CN afforded **7 · CH₃CN** as red crystals (372 mg, 60%). ¹H NMR (C₆D₆): δ 8.11 (d, $J = 7.8$ Hz, 1H, fluorenyl), 7.95 (d, $J = 6.0$ Hz, 1H, fluorenyl), 7.41 (m, 2H, fluorenyl), 7.10 (m, 3H, fluorenyl), 6.95 (t, $J = 6.0$ Hz, 1H, fluorenyl), 5.11 (d, $^1J_{H-P} = 18.0$ Hz, 1H, fluorenyl), 3.64 (s, 3H, N(CH₃)₂), 3.60 (s, 3H, N(CH₃)₂), 3.31 (s, 3H, N(CH₃)₂), 3.22 (s, 3H, N(CH₃)₂), 2.79 (m, 2H, NCH(CH₃)₂), 1.55 (s, 3H, CH₃CN), 0.54 (d, $J = 6.0$ Hz, 6H, NCH(CH₃)₂), -0.22 (d, $J = 6.0$ Hz, 6H, NCH(CH₃)₂). ¹³C NMR (C₆D₆): δ 143.2, 142.4, 137.3, 136.7, 127.1, 120.1, 48.9 (d, $^1J_{-P} = 74.9$ Hz) (C₁₃H₉), 119.0 (CH₃CN), 91.0 (cage C), 48.1 (br) (NCH(CH₃)₂), 50.7, 50.5, 47.6, 47.0 (N(CH₃)₂), 31.9, 23.1, 22.2, 21.0 (NCH(CH₃)₂), 1.29 (CH₃CN). ¹¹B{¹H} NMR (C₆D₆): δ 7.9 (1B), -1.6 (4B), -12.7 (3B), -17.9 (1B). ³¹P{¹H} NMR (C₆D₆): δ 70.6. IR (KBr, cm⁻¹): ν 2536 (vs) (B-H), 1445 (s) (P=O). Anal. Calcd for C₂₆H_{46.5}B₉N_{3.5}OPTi (7 + 0.5CH₃CN): C, 52.02; H, 7.81; N, 8.17. Found: C, 52.11; H, 7.93; N, 7.99.

Preparation of $\{[\eta^1\text{-}\eta^5\text{-}(\text{C}_{13}\text{H}_9)(\text{Pr}_2\text{N})\text{P}(\text{O})(\text{C}_2\text{B}_9\text{H}_{10})]\text{Ti}[(\text{NMe}_2)_2]\}(\eta^6\text{-C}_6\text{D}_6)_2\text{K} \cdot \text{C}_6\text{D}_6$ (8 · C₆D₆). An NMR tube was loaded with **7** (43 mg, 0.07 mmol) and C₆D₆ (0.8 mL). KH (4.0 mg, 0.10 mmol) was added to the NMR tube at room temperature in a glovebox. The reaction mixture was heated at 80 °C for one day, leading to a deep red solution with a gray precipitate. Removal of the precipitate gave a clear red solution. Complex **8 · C₆D₆** was isolated as red crystals after this solution stood at room temperature for 12 h (20 mg, 32%). ¹H NMR (C₆D₆): δ 8.77 (d, $J = 8.1$ Hz, 1H, fluorenyl), 8.65 (d, $J = 8.1$ Hz, 1H, fluorenyl), 8.00 (d, $J = 7.2$ Hz, 1H, fluorenyl), 7.89 (d, $J = 7.2$ Hz, 1H, fluorenyl), 7.77 (t, $J = 8.1$ Hz, 1H, fluorenyl), 7.35 (t, $J = 7.2$ Hz, 1H, fluorenyl), 6.99 (m, 2H, fluorenyl), 3.79 (s, 6H, N(CH₃)₂), 3.43 (s, 6H, N(CH₃)₂), 3.22 (m, 2H, NCH(CH₃)₂), 0.93 (d, $J = 6.9$ Hz, 6H, NCH(CH₃)₂), 0.71 (d, $J = 6.9$ Hz, 6H, NCH(CH₃)₂). ¹¹B{¹H} NMR (C₆D₆): δ 3.9 (1B), -4.4 (3B), -6.6 (1B), -15.2 (3B), -20.8 (1B). ³¹P{¹H} NMR (C₆D₆): δ 54.8. IR (KBr, cm⁻¹): ν 2550 (vs) (B-H), 1431 (m) (P=O). Anal. Calcd for C₃₇H₄₄B₉D₁₂KN₃OPTi (8): C, 56.53; H, 8.72; N, 5.35. Found: C, 56.35; H, 8.53; N, 5.31.

X-ray Structure Determination. All single crystals were immersed in Paratone-N oil and sealed under N₂ in thin-walled glass capillaries. Data were collected at 293 K on a Bruker SMART 1000 CCD diffractometer using Mo Kα radiation. An empirical absorption correction was applied using the SADABS program.²⁰ All structures were solved by direct methods and subsequent Fourier difference techniques and refined anisotropically for all non-hydrogen atoms by full-matrix least-squares calculations on *F*² using the SHELXTL program package.²¹ All hydrogen atoms were geometrically fixed using the riding model. Crystal data and details of data collection and structure refinements are given in Tables 2 and 3. Selected bond distances and angles are compiled in Table 1. Further details are included in the Supporting Information.

Acknowledgment. This work was supported by grants from NSFC/RGC Joint Research Scheme (No. CUHK466/06) and State Key Laboratory of Elemento-Organic Chemistry, Nankai University (Project No. 0314).

Supporting Information Available: Crystallographic data in CIF format for **3**, **4**, **5 · THF**, **6**, **7 · CH₃CN**, and **8 · C₆D₆**. This material is available free of charge via the Internet at <http://pubs.acs.org>.

OM800319W

(20) Sheldrick, G. M. *SADABS: Program for Empirical Absorption Correction of Area Detector Data*; University of Göttingen: Germany, 1996.

(21) Sheldrick, G. M. *SHELXTL 5.10 for Windows NT: Structure Determination Software Programs*; Bruker Analytical X-ray Systems, Inc.: Madison, WI, 1997.